HOW IMPORTANT IS SMALL-SCALE GEOCHEMICAL VARIABILITY TO CONSTRAINING SOURCES AND PROCESSES?

Jade M. Bowers, Darin M. Schwartz, V. Dorsey Wanless
Department of Geosciences, Boise State University, Boise, 83725

How valid is the assumption of homogeneity?

Pyroclasts hold information about eruption and magma dynamics

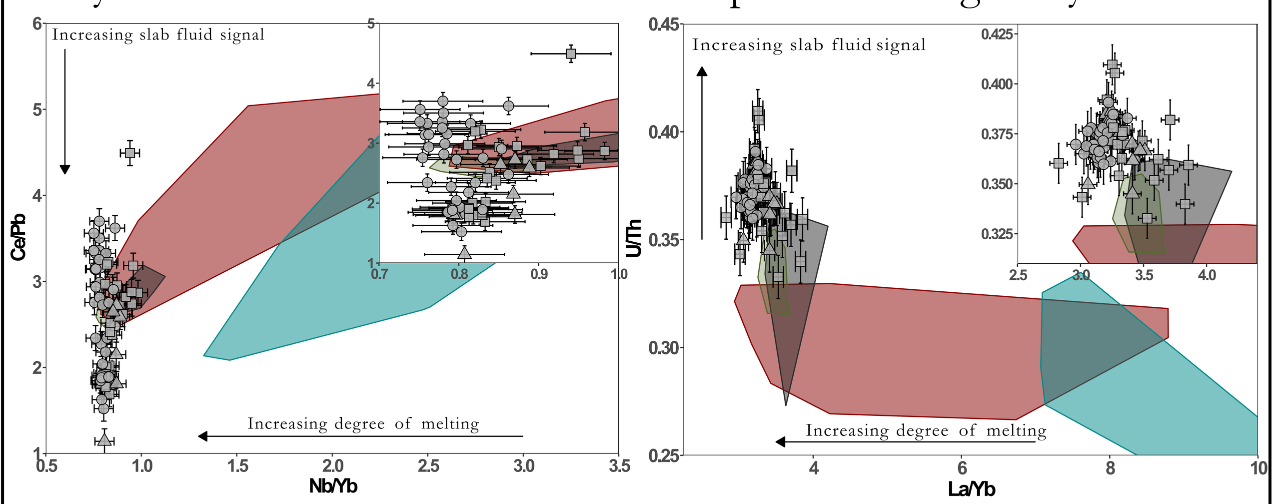

Figure 1. Curacautín samples define a vertical trend with variation in Ce/Pb and U/Th, potentially reflecting mixing between a high slab fluid source and an end member with less slab fluid influence, and the lowest Nb/Yb and La/Yb of the CSVZ (red), TSVZ (blue), Villarrica (green), and other published Llaima (gray) data, reflecting the highest degrees of melting or derivation from a more depleted source material.

Q: What does an average mean?

Q: Is there hidden variability in the pyroclasts?

Hypothesis

Individual pyroclasts in a sampling horizon are chemically heterogeneous

Materials and Methods

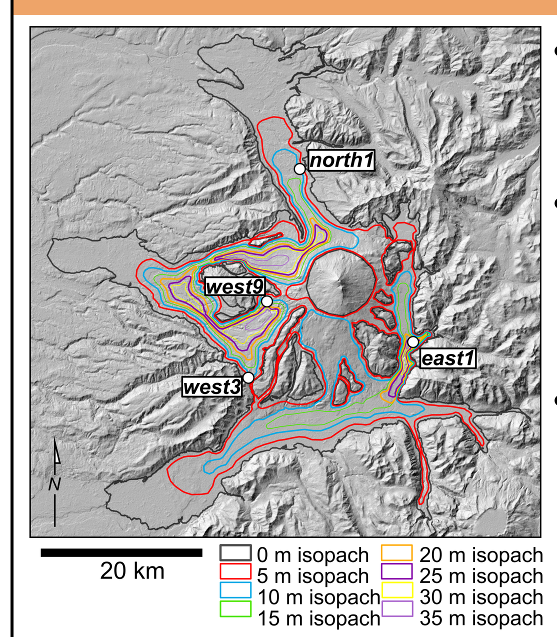

- ~12.6 ka Curacautín ignimbrite (CI) of Llaima Volcano (Chile) (Marshall et al. 2021, JVGR)
- 3.5-4.5 km³ DRE of pristine, vertically extensive exposures of basaltic andesite pyroclastic material (Marshall et al. 2021, JVGR)
- No visible evidence of mingling

Figure 2. Isopach map of the CI volume estimate modified from Marshall et al. (2021) with outcrop locations of targeted sampling horizons overlain. JB21 is from east1 (**a**), JB29 is from west 9 (**b**), JB45 is from north1 (**c**), and L43 is from west3 (**d**).

Selected **four** depositional horizons

1. JB29 - base of ignimbrite

2. JB21 - top of ignimbrite

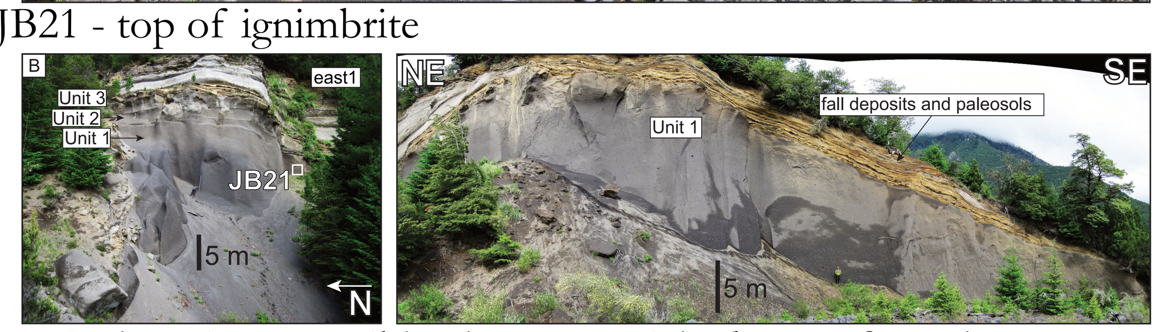

3. JB45 - least incompatible-element enriched, top of north1

4. L43 - most incompatible-element enriched

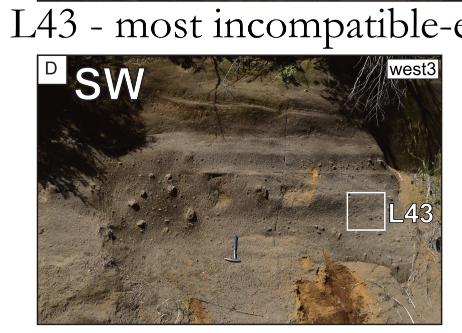

Figure 3. Outcrop photos of **a** West9, **b** East1, **c** North1, and **d** West3. Sample horizons targeted in this study are indicated in their respective outcrop photos (white boxes) with the exception of JB45 which is out of the extent of the photo (**c**).

- Randomly selected 10 pyroclasts from each sampling horizon
- Developed 5-mg sample prep procedure for trace element characterization via solution-based ICPMS

Acknowledgments

This work was made possible by the National Science Foundation EAR grant 1831143. A special thank you to Pedro Valdivia for his help with sample collection and colleagues in the BSU Isotope Geology Lab.

> 75% of elements record true variability

χ^2 test for variance

$$\chi^2 = \frac{(n-1)S^2}{\sigma_R^2} \longrightarrow S^2 = \frac{\sigma_R^2}{\chi^2(n-1)}$$

σ_t = est. of true standard deviation

$\sigma_t^2 = \sigma_o^2 - \sigma_r^2$

σ_t/σ_r = signal to noise ratio

variability ≠ only random error: $\sigma_t/\sigma_r \geq 1.83$

	JB21	JB29	JB45	L43
TiO_2	2.7	13.53	8.39	2.58
Al_2O_3	3.49	1.33	1.72	
FeO	7.81	9.18	10.13	2.83
MnO	2.89	2.48	4.82	21.52
MgO	6.92	2.43	3.99	1.03
CaO	11.48	5.25	9.86	1
Na_2O	6.86	4.16	7.93	3.13
K_2O	19.46	14.44	31.27	16.02
P_2O_5	20.72	13.5	29.74	3.92
Ni	106.9	25.6	45	94.99
Cr	87.34	105.74	41.61	265.04
V	37.89	13.46	24.32	5.47
Sc	2.18	1.77	2.42	

	JB21	JB29	JB45	L43
La	12.77	4.16	16.85	4.89
Ce	8.72	2.7	10.56	1.94
Pr	10.8	3.61	13.46	2.96
Nd	40.41	15.37	54.07	11.96
Sm	10.66	4.12	13.44	3.38
Eu	5.3	1.97	6.5	1.46
Gd	23.07	9.27	28.89	7.73
Tb	6.73	2.63	8.58	1.96
Dy	5.21	2.12	6.46	1.44
Ho	5.89	2.39	7.43	1.78
Er	5.82	2.18	7.34	1.63
Tm	9.89	4.21	12.6	2.81
Yb	6.24	2.57	8.08	0.91
Lu	3.81	1.43	4.97	1.03

	JB21	JB29	JB45	L43
Ba	5.54	2.92	7.73	3.49
Th	5.93	2.35	6.56	
Nb	18.42	7.4	24.29	2.22
Y	6.87	2.87	7.9	2.06
Hf	13.38	4.41	16.92	2.35
Ta	6.53	2.03	8.47	1.25
U	16.52	13.65	17.62	17.76
Pb	7.97	1.8	14.33	11.03
Rb	14.4	14.27	20.39	9.4
Cs	18.45	4.64	15.42	7.1
Sr	3.84	4.62	6.29	0.83
Zr	6.42	2.41	8.8	0.94
Zn	2.54	4.33	4.53	3.88

	JB21	JB29	JB45	L43
Zr/Y	1.27	1.32	1.46	1.29
La/Sm	1.68	1.61	1.87	1.67
Nb/Zr	2.16	2.03	2.16	2.09
Rb/Y	3.72	3.56	4.06	4.02
Th/Zr	3.12	2.86	3.05	2.64
Nb/Y	2.4	2.32	2.66	2.34
Nb/Yb	2.39	2.31	2.81	2.34
Ce/Pb	2.15	2.03	2.17	2.07
U/Th	4.5	5.04	3.98	5.03
Ba/Th	3.72	3.87	3.58	4.95
La/Yb	1.73	1.67	2.01	1.7

true variability
random error

Figure 4. Outcomes of χ^2 test for variance. The null hypothesis tested was that all variability is due to random error (analytical uncertainty). Based variable relationships and inequalities that are true if the null hypothesis is accepted, we determined that a signal to noise ratio greater than 1.83 would reject the null hypothesis. Less than 15% of the calculations accepted the null hypothesis (red or grey boxes). Grey boxes are elements where standard deviation of the observations was less than 1σ analytical error.

Compositional variability between pyroclasts exists

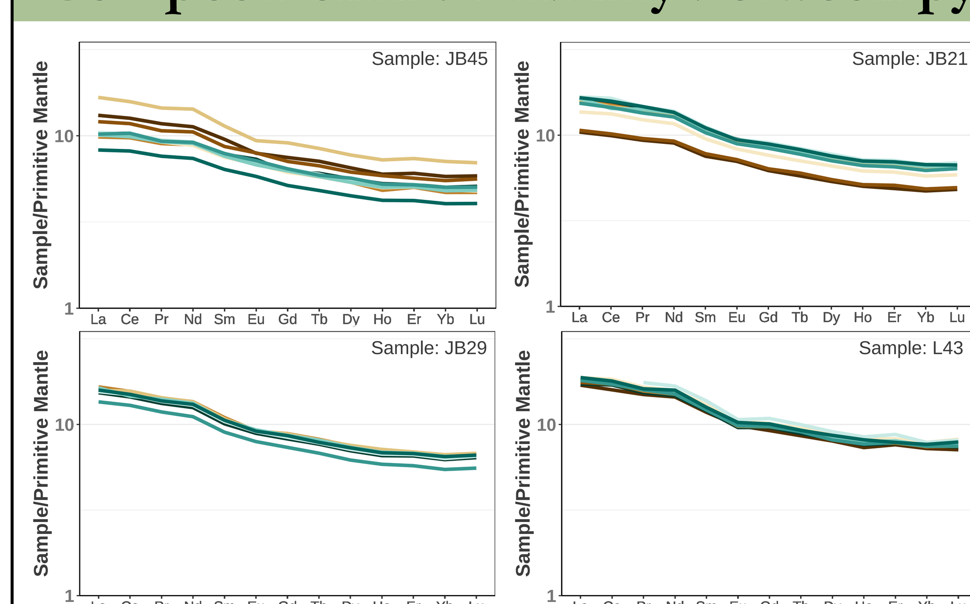

Figure 5. REE diagrams for each sampling horizon targeted, each color represents composition of a single pyroclast from the sampling horizon. Some sampling horizons are relatively homogeneous in REE concentrations (L43 and JB29 with the exception of one pyroclast) while JB45 and JB21 are heterogeneous. REE_{sum} varies between the pyroclasts in the sampling horizon but slope is relatively constant indicating fractional crystallization as a likely source for variability in REE concentrations.

Variability in one sampling horizon is greater than in the entire stratigraphic section

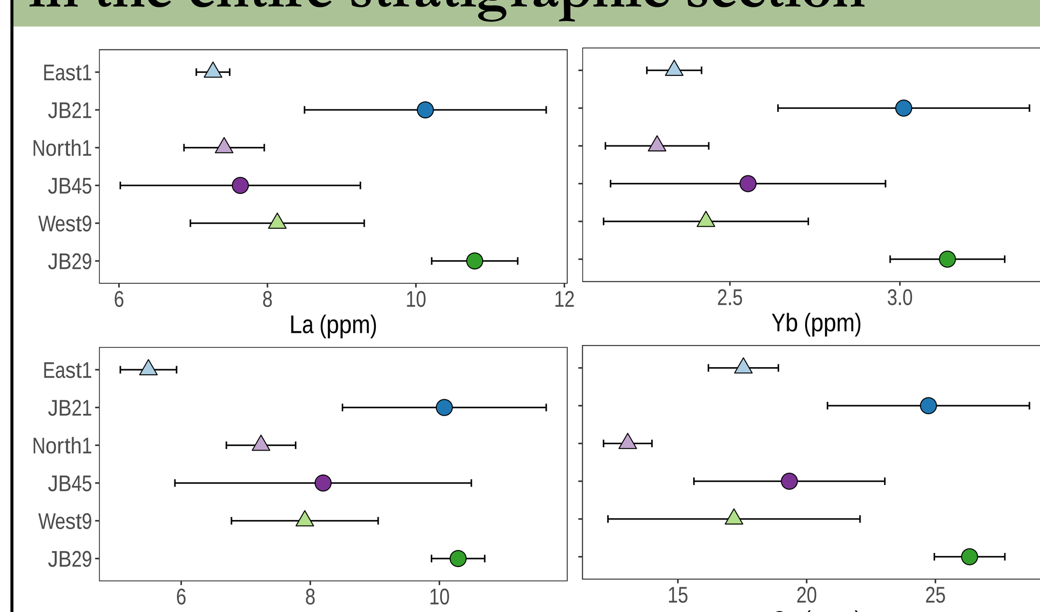

Figure 6. Comparison of variability at outcrop scale to variability at a single point in the outcrop. Variability is compared by calculating the mean and standard deviation of the two populations.

Potential causes of variability

- Batches of magma with different mantle (or subduction component) melt sources
- Batches (or pockets) of magma that experienced variable degrees of fractionation
- Variable incorporation of microscopic lithics (mafic extrusives or felsic intrusives)

Melting different sub-CSVZ mantle sources

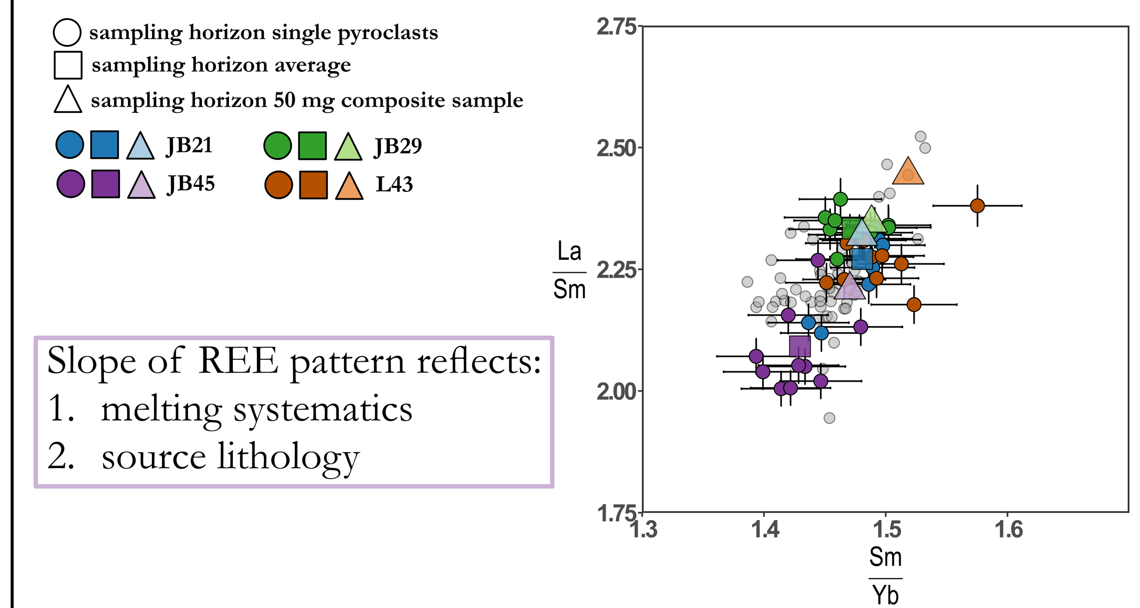

Slope of REE pattern reflects:
1. melting systematics
2. source lithology

Previous CSVZ regional studies proposed less LREE-enriched form from ambient asthenospheric mantle (**peridotite**) and more LREE-enriched include partial melts of mantle lithosphere (**pyroxenite**).

Partial melting of peridotite and pyroxenite

- REE concentrations of E-MORB mantle source
- Calculated compositions of primary melts of:
  1. **Peridotite** (60% olv, 20% opx, 15% cpx, and 5% spl)
  2. **Pyroxenite** (20% olv, 40% opx, 30% cpx, and 10% spl)
  3. **Garnet pyroxenite 1** (10% olv, 30% opx, 50% cpx and 10% grnt)
  4. **Garnet pyroxenite 2** (10% olv, 30% opx, 55% cpx and 5% grnt)

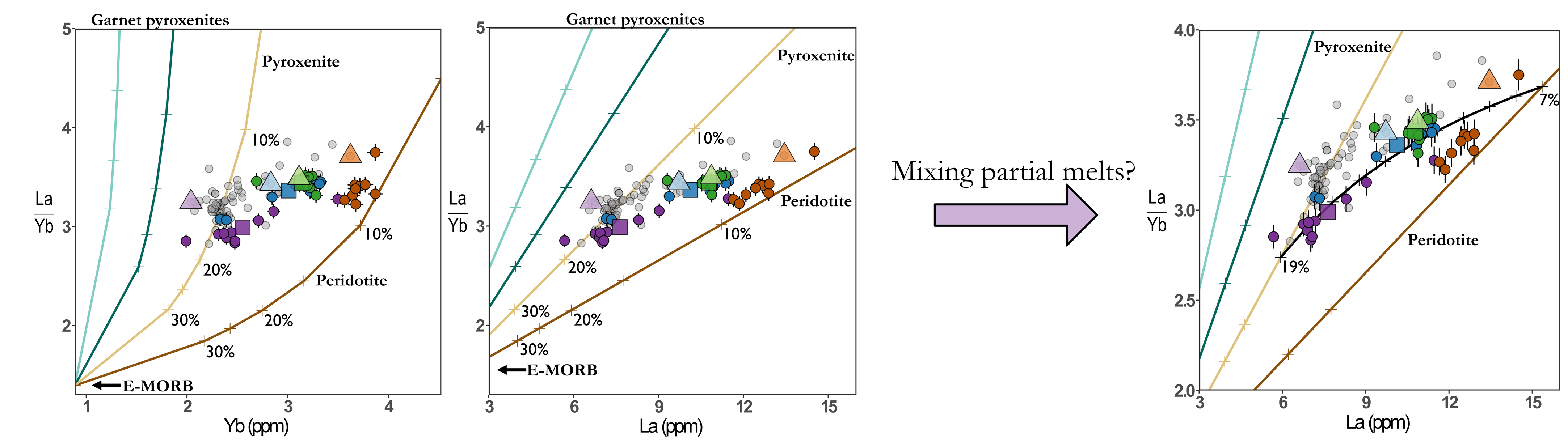

Mixing partial melts?

Varying degree of fractional crystallization

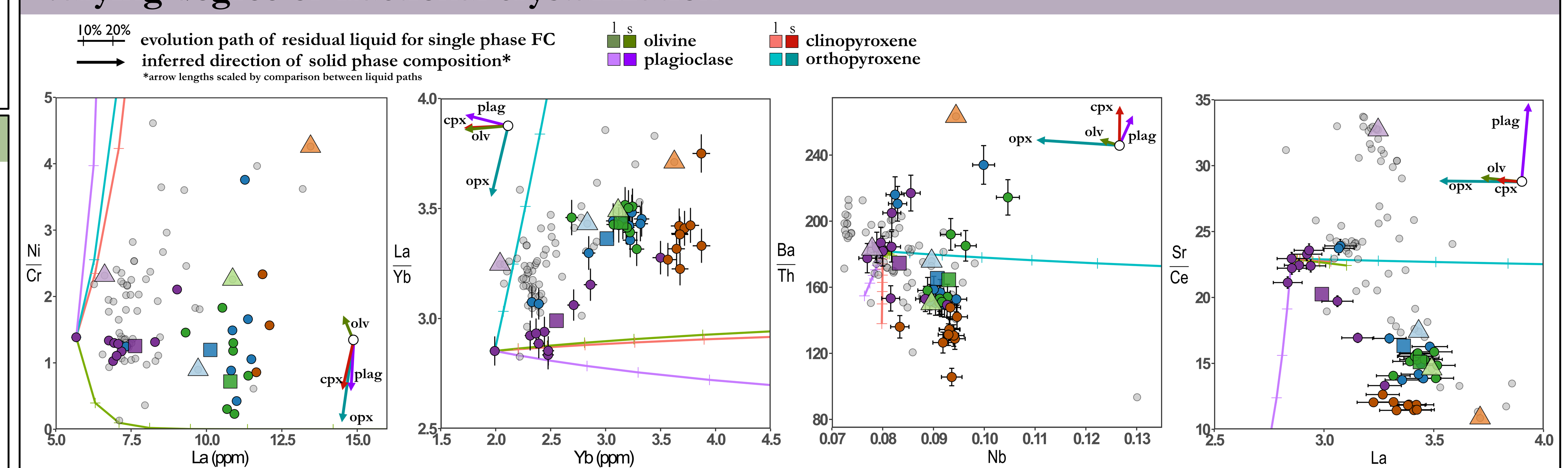

- Multi-phase fractional crystallization can explain some observed variability
- Accumulation of phases (microlites?) can explain variability trending opposite of liquid evolution or in direction of mixing with hypothesized solid phase

Subduction-component or Assimilation

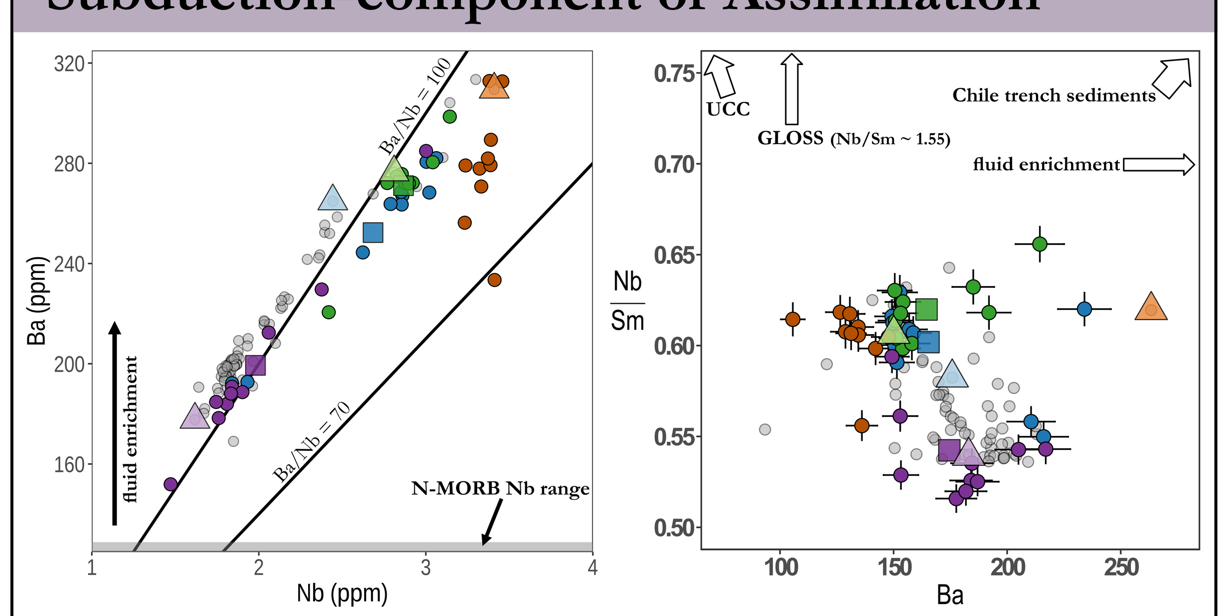

- Nb and Nb/Sm at level of many N-MORBs
- Fluid-mobile Ba abundances are orders of magnitude higher
- Derived from mantle sources enriched primarily by fluids or highly-fluid rich melts
- L43 50-mg most incompatible-element enriched sample
  - Highest $^{87}Sr/^{86}Sr$ and lowest $^{144}Nd/^{143}Nd$
  - Continental Crust: Ba/Nb ~ 50

Conclusions

- Small-scale sampling detected previously unseen variability
- Four sampling horizons cover compositional range of all 68 CI samples from 17 different outcrops
- One sampling horizon spans the CI compositional range
- End member sampling horizons cluster together further constraining end member composition
- Composite samples are a weighted mean not an average
- Potential causes of variability between pyroclasts
  - Mixing of partial melts of peridotite (asthenospheric mantle) and pyroxenite (mantle lithosphere) could explain variability in REE ratios
  - Different percentages of fractional crystallization of varying proportions of primary phases and phase accumulation
  - Phenocrysts are removed before analysis, could microlites migrate in the magma during ascent?
  - Ba/Nb is consistent suggesting no mixing between variably fluid enriched melts
  - L43 trends toward lower Ba/Nb more similar to CC
    - Assimilation or microscopic lithics?